A Molecular-Statistical Approach to Hyperelasticity of Elastomer Materials

M. Klüppel, J. Schramm
Deutsches Institut für Kautschuktechnologie e. V.,
Eupener Straße 33, 30519 Hannover, FRG

0. Abstract

A micro-mechanical concept of hyperelasticity of reinforced rubbers is presented that combines a generalized non-Gausian tube model of rubber elasticity with a damage model of stress-induced filler cluster breakdown. The functional integral formulation of rubber elasticity is reviewed, briefly, and compared to the classical Mooney-Rivlin- and Inverse-Langevin approaches of rubber elasticity. On this basis, hydrodynamic reinforcement by rigid, self-sinilar filler clusters is considered that allows for a quantitative description of stress softening by means of a strain or pre-strain dependent hydrodynamic amplification factor, respectively. Thereby, the high hysteresis of reinforced rubber is referred to a irreversible break down of filler clusters during the first deformation cycle. It is shown that the developed concept is in fair agreement with uniaxial stress-strain data of unfilled NR-samples of variable cross-link density and carbon black filled E-SBR- and EPDM-samples.

1. Introduction

The micro-mechanical modellization of quasi-static stress-strain properties of reinforced elastomers involves different influences and mechanisms that have been discussed by a varity of authors, but in most cases only on a qualitative level. Beside the action of the entropy elastic polymer network that is quite well understood on a molecular-statistical basis [1,2], the impact of filler particles on stress-strain properties is of high importance, but so far the micro-mechanical effects of the filler are not totally understood [3,4]. On the one hand side the addition of hard filler particles leads to a stiffening of the rubber matrix that can be described by a hydrodynamic strain amplification factor [5-7]. On the other hand side the constraints introduced into the system by filler-polymer bondings result in a decreased network entropy and hence, the free energy that equals the negative entropy times the temperature increases linear with the effective number of network junctions [8,9]. A further effect can be obtained from the formation of filler clusters or a filler network due to strong attractive filler-filler bondings [3,4,6-10].

A complication for the modellization of reinforced rubbers is the pronounced stress softening during quasi-static deformations that is also termed Mullins effect due to the extensive measurements carried out by Mullins [11-13]. Dependent on the history of straining, e.g. the extent of previous stretching, the rubber material undergoes an almost permanent change that alters the elastic properties and increases hysteresis, drastically. Most of the softening occurs in the first deformation and after a few deformation cycles the rubber approaches a steady state with a constant stress-strain behavior. The softening is usually only present at deformations smaller than the previous maximum. An example of stress softening is shown in Fig. 1, where the maximum strain is increased, successively, from one uniaxial stretching cycle to the next.

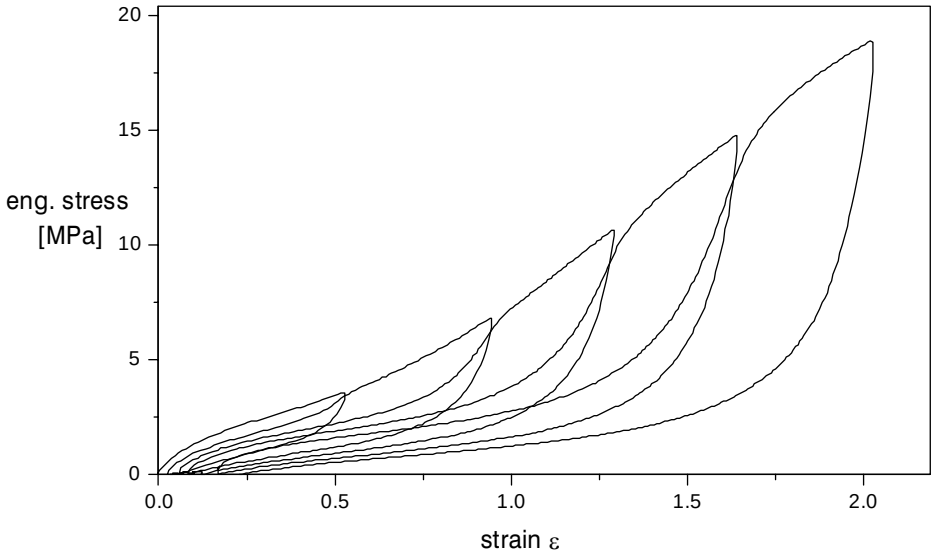

Fig. 1: Quasi-static stress-strain cycles with successively increasing maximum strain for E-SBR-samples filled with 80 phr N 339.

The softening has been attributed to breakdown or slippage [14-17] and disentanglements [18] of bonds between filler and rubber, while other authors assumed that a strain-induced crystallization-decrystallization [19,20] or a rearrangement of network chain junctions in filled systems [13] is responsible for the large hysteresis. A quantitative description of stress-induced breakdown or separation of network chains from the filler surface is given in Ref. [15] where a complete macroscopic constitutive theory is derived on the basis of statistical mechanics. However, this kind of interpretation of stress softening ignores the important experimental result of Haarwood et al. [19,20], who showed by a simple mastering procedure that stress softening is related to hydrodynamic strain amplification due to the presence of the filler. A plot of stress in second extension vs. ratio between strain

and pre-strain of natural rubber filled with a varity of carbon blacks yields a single master curve [13,19].
It's the aim of this paper to present a quantitative molecular-statistical model of hyperelasticity of filler reinforced rubbers that considers stress softening as a result of strain amplification by rigid filler clusters of variable size. In the first part an advanced concept of rubber elasticity is considered that combines the Edwards-Vilgis approach of finite network extensibility with a topological constraint contribution in a generalized non-Gaussian tube-model for unfilled rubbers. In the second part of the paper we will develop a micro-mechanical picture of filler cluster breakdown during quasi-static straining. It yields a damage model for the description of stress softening by means of a hydrodynamical amplification factor that depends on the applied strain during the first deformation of the virgin sample or maximum pre-strain in the following cycles, respectively. In the third part we will present experimental results on filled and unfilled samples. In particular, we will show how the parameters of the model can be estimated by a fitting procedure for the pre-strained filled samples.

2. A generalized tube model of rubber elasticity

The classical concepts of rubber elasticity consider so called phantom networks of freely fluctuating chains that are not influenced by any constraining potential appart from the cross-links [1,2]. This is a rough approximation, because in typical elastomer networks the chains cannot move freely due to the large degree of chain interpenetration. It restricts the chain fluctuations by packing effects that result from the inability of the chains to pass through its neighbours. The topological constraints on a single chain (packing effects) can be described by a tube model, i.e. a harmonic potential that forces the chain to remain in a virtuel tube around its mean position. In the case of strong topological constraints, relevant for highly molecular rubbers, the elastic free energy density can be expressed as [1]:

$$W \equiv W_c + W_e = \frac{G_c}{2}\left(\sum_{\mu=1}^{3}\lambda_\mu^2 - 3\right) + 2G_e\left(\sum_{\mu=1}^{3}\lambda_\mu^{-1} - 3\right) \qquad (1)$$

where λ_μ is the strain ratio in direction of the main axis system, G_c is the elastic modulus that corresponds to the crosslink constraints and G_e corresponds to the topological tube constraints:

$$G_c = \frac{1}{2}\upsilon_c k_B T = \frac{\upsilon_s l_s^2 k_B T}{2 < R_o^2 >} \qquad (2)$$

$$G_e = \frac{\upsilon_s l_s^2 k_B T}{4\sqrt{6}\, d_o^2} \tag{3}$$

Here, υ_c is the chain density, υ_s is the density of statistical segments, l_s is the length of statistical segments, $<R_o^2>$ is the average end-to-end distance of chains in the underformed state, d_0 is the tube radius (mean fluctuation radius of chain segments), k_B is the Boltzmann constant and T is temperature.

Equ. (1) with the two elastic moduli G_c and G_e is closely related to the semi-empirical Mooney-Rivlin equation with constants C_1 and C_2:

$$W = C_1\left(\sum_{\mu=1}^{3}\lambda_\mu{}^2 - 3\right) + C_2\left(\sum_{\mu=1}^{3}\lambda_\mu{}^{-2} - 3\right) \tag{4}$$

It relates the elastic energy to the first and second deformation invariants, i.e. the bracket terms of Equ. (4). Obviously, Equ. (1) does not envolve the second invariant. This is a direct consequence of a non-affine tube deformation law that leads to Equ. (1). The modified assumption of affine tube deformations reproduces the Mooney-Rivlin Equ. (4). This makes clear that the a-priori postulate of affine deformations on all length scales as applied in continuum mechanics, e.g. the Mooney-Rivlin theory, may not be fulfilled in molecular-statistical approaches of rubber elasticity.

So far, all considerations are valid in the Gaussian limit of infinite long chains. For that reason no singularity appears in the elastic free energy density Equ. (1) that could reflect the finite extensibility of real polymer networks. A singularity can be obtained if the inverse Langevin approximation is used instead of the Gaussian distribution function for the end-to-end distance of network chains [21]. Thereby, it is sufficient to consider the modifications of the cross-link term W_c in Equ. (1), because the topological constraint term W_e goes to zero at large strains ($W_e \sim \lambda_\mu^{-1}$), where the finite extensibility becomes significant [22-24]. This argument is confirmed by recent molecular-statistical investigations of tube like network models based on non-Gaussian network chains, which show that the action of tube constraints becomes weaker in the case of predominance of finite chain extensibility [25,26]. The simplest way to obtain a singularity for the free energy is the modification of Equ. (1) as proposed by Edwards and Vilgis [2]:

$$W_c = \frac{G_c}{2}\left\{\frac{\left(\sum_{\mu=1}^{3}\lambda_\mu^2 - 3\right)\left(1-\frac{T_e}{n_e}\right)}{1-\frac{T_e}{n_e}\left(\sum_{\mu=1}^{3}\lambda_\mu^2 - 3\right)} + \ln\left(1-\frac{T_e}{n_e}\left(\sum_{\mu=1}^{3}\lambda_\mu^2 - 3\right)\right)\right\} \qquad (5)$$

Here, T_e is the Langley trapping factor [27] and n_e is the segment number of chains between successive entanglements. The singularity of W_c is found for $n_e/T_e=\sum \lambda_\mu^2$ - 3, i.e. if the chains between successive trapped entanglements are fully stretched out. This makes clear that the approach in Equ. (5) characterizes trapped entanglements as some kind of physical cross-links (slip-links) that dominate the extensibility of the network due to the larger number of entanglements as compared to chemical cross-links. We note, that this gives a less pronounced upturn of stress-strain curves as compared to the classical inverse Langevin approach, which can be related to the more flexible response of trapped entanglements as compared to chemical cross-links.

The final expression for the elastic free energy that considers finite extensibility together with tube constraints is found from a combination of Equ. (5) with the second term of Equ. (1):

$$W = \frac{G_c}{2}\left\{\frac{\left(\sum_{\mu=1}^{3}\lambda_\mu^2 - 3\right)\left(1-\frac{T_e}{n_e}\right)}{1-\frac{T_e}{n_e}\left(\sum_{\mu=1}^{3}\lambda_\mu^{-2} - 3\right)} + \ln\left(1-\frac{T_e}{n_e}\left(\sum_{\mu=1}^{3}\lambda_\mu^2 - 3\right)\right)\right\} + 2G_e\left(\sum_{\mu=1}^{3}\lambda_\mu^{-1} - 3\right) \qquad (6)$$

In the limit $n_e \to \infty$ the Gaussian formulation of infinite long chains Equ. (1) is recovered. From Equ. (6) the engeneering stress $\sigma_{o,\mu}$ that relates the force f_μ in direction μ to the underformed cross section $A_{o,\mu}$ is found by differenciation $\sigma_{o,\mu} = \partial W/\partial\lambda_\mu$. In the case of uniaxial extension with $\lambda_1=\lambda$, $\lambda_2=\lambda_3=\lambda^{-1/2}$ this yields:

$$\sigma_{0,1} = G_c\left(\lambda-\lambda^{-2}\right)\left\{\frac{1-T_e/n_e}{\left(1-\frac{T_e}{n_e}(\lambda^2+2/\lambda-3)\right)^2} - \frac{T_e/n_e}{1-\frac{T_e}{n_e}(\lambda^2+2/\lambda-3)}\right\} + 2G_e(\lambda^{-1/2}-\lambda^{-2}) \qquad (7)$$

With this equations the model parameters G_c, G_e and T_e/n_e can be found from fittings to experimental stress-strain curves.

3. Stress softening by stress-induced filler cluster breakdown

For an extension of Equs. (6) and (7) to filler reinforced rubbers we have to consider hydrodynamic effects of filler particles and rigid filler clusters. The filler clusters result from an aggregation process in the rubber matrix subject to strong physical bondings between filler particles. Possible aggregation mechanisms are percolation or kinetical aggregation that both lead to a selfsimilar cluster structure [28]. We assume that due to the stabilizing bound rubber layer at the cluster surface, the strength of the filler clusters is quite high and hence, part of these clusters survive up to large deformations. With increasing strain of a virgin sample, a stress-induced successive breakdown of filler clusters takes place, during which the size of the clusters decreases. This process is almost irreversible, because for quasi-static experiments the gaps between broken filler clusters fill up with polymer that is expected to be strongly bonded to the filler surface and hence, hinders the reaggregation of the clusters when the stress relaxes during the backcycle of straining. It means that the cluster size that is reached at the maximum strain of the first cycle remaines fixed for a long time periode and almost no change of the cluster size takes place during the following cycles as long as the maximum pre-strain is not exceeded. If a larger strain is applied in a following cycle, a further breakdown of the clusters appears that is then frozen in the next cycles. This is the basic mechanism of stress softening in filler reinforced rubbers. It leads to the characteristic stress-strain behavior shown in Fig. 1, if the hydrodynamic reinforcement of the clusters is considered.

Hydrodynamic reinforcement can be described by a strain amplification factor X that relates the microscopic intrinsic strain $\lambda = 1+\varepsilon_o$ of the rubber to the macroscopic external strain $\Lambda = 1+\varepsilon$ of the sample ($X = \varepsilon_o/\varepsilon$). As mentioned above, the use of a strain amplification factor X appears appropriate for a modellization of the stress-strain behavior of pre-strained reinforced rubbers if X is coupled to the previous straining ε_{max} of the sample. Then the stress-strain curves in the second or third cycle can be described by a constant strain amplification factor $X_{max}=X(\varepsilon_{max})$ that depends on the pre-strain ε_{max} as long as the applied external strain ε is smaller than ε_{max}. It means that Equs. (6) and (7) remain valid if the intrinsic strain λ is expressed by the external strain ε as follows:

$$\lambda = 1 + X_{max}\,\varepsilon \qquad \text{for } \varepsilon < \varepsilon_{max} \qquad (8)$$

If in a following cycle the sample is strained to a higher value $\varepsilon'_{max} > \varepsilon_{max}$, then the filler clusters break further down and the hydrodynamical amplification factor $X_{max}' = X(\varepsilon'_{max})$ that is representative for the next cycles decreases ($X_{max}' < X_{max}$). In the following we will consider a quantitative model that describes the dependence $X_{max} = X(\varepsilon_{max})$ for selfsimilar filler clusters. It equals the dependence $X=X(\varepsilon)$ during the first straing of the virgin sample and hence we can restrict to this case.

Hydrodynamic reinforcement by selfsimilar, rigid filler clusters was modellized on the basis of a path integral formalism by Huber et al. [7], who found the following scaling law for the hydrodynamic amplification factor in the case of high filler concentrations ϕ with overlapping neighbouring clusters:

$$X = 1 + \text{const.} \left(\frac{\xi}{a} \right)^{d_w - d_f} \phi^{\frac{2}{3-d_f}} \qquad (9)$$

Here, ξ is the cluster size, *a* is the particle size, d_f is the fractal dimension and d_w the anomalous diffusion exponent of the clusters. It shows that the strain amplification factor increases with filler concentration and cluster size according to a power law with an exponent that depends on the fractal structure of the clusters.

This result Equ. (9) can be combined with a concept of stress-induced cluster breakdown. In a first approach one may assume an exponential decrease of the cluster size with increasing strain:

$$\frac{\xi(\varepsilon)}{a} = \frac{\xi_o}{a} \exp(-\alpha(1+\varepsilon)) + 1 \qquad (10)$$

The second summand ensures the right infinite strain limit $\varepsilon \to \infty$, where all clusters are broken and the cluster size should equal the particle size. The exponent α in this model is purely emprical and may depend on the strength of the clusters or the elastic modulus of the rubber.

By inserting Equ. (10) into Equ. (9) we find a strain dependent amplification factor $X(\varepsilon)$ that relates the external strain $\Lambda = 1+\varepsilon$ to the internal strain λ of the polymer chains. Then, instead of Equ. (8) with a constant hydrodynamic amplification factor X_{max}, relevant for pre-strained samples, the following equation results for non-strained virgin sample:

$$\lambda = 1 + X(\varepsilon)\varepsilon = 1 + X_\infty \varepsilon + (X_o - 1)\exp(-z(1+\varepsilon))\varepsilon \qquad (11)$$

The exponent z is given by $z = \alpha\,(d_w - d_f)$ and abreviations for the zero and infinite strain limits for the amplification factor X_o and X_∞ are used:

$$X_o = 1 + \text{const.}\left(\frac{\xi_o}{a}\right)^{d_w - d_f}\,\phi^{\frac{2}{3-d_f}} \qquad (12)$$

$$X_\infty = 1 + \text{const.}\,\phi^{\frac{2}{3-d_f}} \qquad (13)$$

The stress-strain behavior of filler reinforced virgin rubber samples is described by Equs. (6) and (7) together with Equ. (11), while for pre-strained samples Equ. (8) has to be applied. Then, the hydrodynamic amplification factor X_{max} fulfills:

$$X_{max} = X_\infty + (X_o - 1)\,\exp(-z(1+\varepsilon_{max})) \qquad (14)$$

The difference between $X(\varepsilon)$ and X_{max} corresponds to the pronounced stress softening of reinforced rubbers. It results from the almost irreversibly breakdown of filler clusters during the first deformation cycle.

4. Results and discussion

Fig. 2 shows uniaxial stress-strain results of unfilled NR-samples at 100 °C that are cross-linked with a variable amount of TMTD. The solid lines correspond to fittings according to Equ. (7) that are in good agreement with the experimental data. The dependence of estimated fitting parameters on TMTD-concentration is shown in Fig. 3. As expected from Equ. (2) and (3) the cross-link modulus G_c increases with increasing TMTD-concentration, while the topological constraint modulus approaches a plateau value that is characteristic for the constant entanglement density of the rubber, independent of cross-link density. The third parameter n_e/T_e decreases with increasing TMTD-concentration that can be related to an increase of the trapping factor T_e with rising cross-link density. Hence, the behavior of the model parameters for the unfilled NR-samples is well understood.

Fig. 4 shows the uniaxial stress-strain behavior of E-SBR-samples that are filled with 40 phr N339. Data for the virgin sample in first extension and for differently pre-strained samples in second extension are shown. The cross-linking system is kept fixed for all samples (1.8 phr sulfur, 1.2 phr CBS, 0.4 phr DPG). Beside the experimental date, fitted curves are shown as solid lines for the pre-strained samples according to Equs. (7) and (8). The fitting parameters for the rubber matrix G_c, G_e and n_e/T_e are hold constant for the differently pre-strained (and virgin) samples (compare

insert of Fig. 4). The impact of pre-straining is modellized by the amplification factor X_{max}. Obviously, the fittings for the pre-strained samples with only one variable parameter X_{max} that considers the hydrodynamic reinforcement of differently frozen filler cluster structures are fairly well.

The dependence of the fitting parameter X_{max} on pre-strain ε_{max} is demonstrated in Fig. 5, where according to Equ. (14) a half-logarithmic plot is chosen. The unknown parameter X_∞ that appears on the ordinate of Fig. 5 is obtained from a least square fit to Equ. (14). We note that, due to the physical meaning, all X-parameters must be larger than one. This condition is fulfilled for the fitted value $X_\infty = 1.35$ and $X_0 = 12.9$ that is obtained from the axis intersection of the regressin line. Furthermore, the exponent $z = 0.56$ is found from the slope. With these three parameters that describe the hydrodynamic reinforcement of successively broken filler clusters with increasing strain, a simulation of the first extension of the virgin sample is obtained if Equ. (7) is applied together with Equ. (11). This is shown as dashed line in Fig. 4 and confirms the developed micro-mechanical concept of stress-softening.

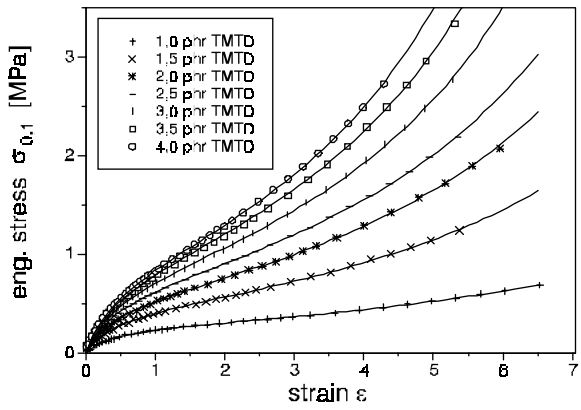

Fig. 2: Stress-strain data and fittings (solid lines) of NR-Samples at 100°C for a varity of cross-linker concentrations TMTD

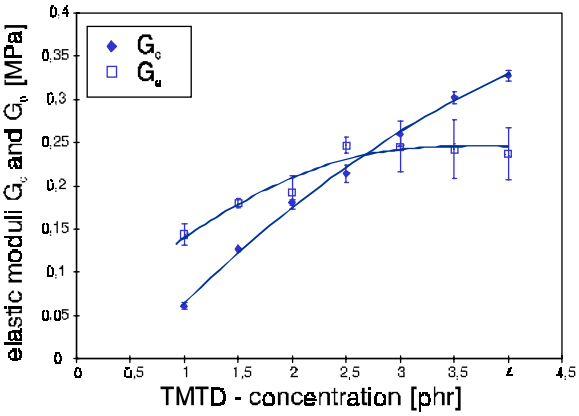

Fig. 3: Estimated fitting parameters G_c and G_e vs. TMTD-concentration from the fitttings in Fig. 2

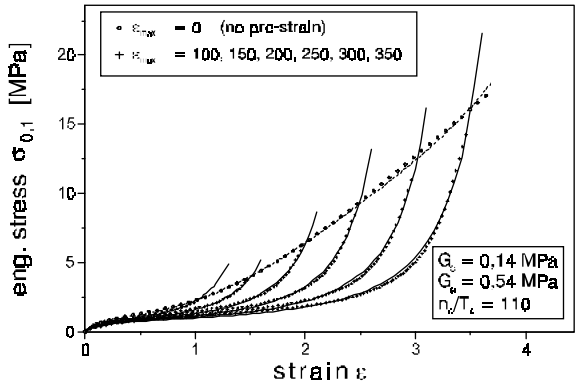

Fig. 4: Stress-strain data and fittings (solid lines) of E-SBR samples filled with 40 phr N339 in the first (o) and second (+) extension at different pre-strains ε_{max}. Dashed line: Prediction of Equs. (7) and (11) with parameters from Fig. 5.

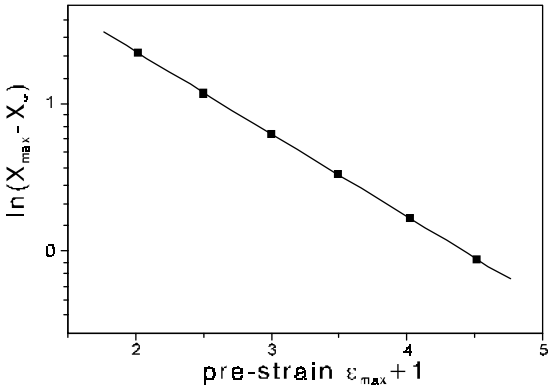

Fig. 5: Plot of $\log(X_{max}-X_z)$ vs. pre-strain $\varepsilon_{max}+1$ from the fits in Fig. 4. $X_z = 1.35$ is estimated from the condition of minimum standard deviation of the regression line that yields $X_0 = 12.9$ and $z = 0.56$ (Equ.(14)).

Literature:

[1] G. Heinrich, E. Straube and G. Helmis, Adv. Polym. Sci. **85,** 33 (1988)
[2] S. F. Edwards and T. A. Vilgis, Rep. Prog. Phys. **51**, 243 (1988); Polymer **27**, 483 (1986)
[3] A. I. Medalia, Rubber Chem. Technol. **46**, 877 (1973); **51**, 437 (1978)
[4] J. B. Donnet, R. C. Bansal and M.-J. Wang, Eds., "Carbon Black Science and Technology", Marcel Dekker Inc. N.Y., Basel, Hongkong (1993)
[5] E. Guth and O. Gold, Phys. Rev. **53**, 322 (1938)
[6] M. Klüppel and G. Heinrich, Rubber Chem. Technol. **68**, 623 (1995)
[7] G. Huber, PhD-Thesis, University Mainz, Germany (1997)
[8] G. Heinrich and T. A. Vilgis, Macromolecules **26**, 1109 (1993)
[9] U. Eisele and H.-K. Müller, Kautsch. Gummi Kunstst. **43**, 9 (1990)
[10] A. R. Payne, J. Appl. Polym. Sci. **6**, 57 (1962); **7**, 873 (1963); **8**, 2661 (1965); **9** 2273, 3245 (1965)
[11] L. Mullins, Rubber Chem. Technol. **21**, 281 (1948)
[12] L. Mullins and N. R. Tobin, Rubber Chem. Technol. **30**, 355 (1957)
[13] L. Mullins, in G. Kraus, Ed., "Reinforcement of Elastomers", Intersc. Publ., N. Y., London, Sydney (1965)
[14] F. Bueche, J. Appl. Polym. Sci, **4**, 107 (1960); **5,** 271 (1961)
[15] S. Govindjee and J. Simo, J. Mech. Phys. Solids **39**, 87 (1991); **40**, 213 (1992)
[16] E. M. Dannenberg, Rubber Chem. Technol. **47**, 410 (1974)
[17] Z. Rigbi, Adv. Polym. Sci. **36**, 21 (1980)
[18] G. R. Hamed and S. Hatfield, Rubber Chem. Technol. **62**, 143 (1989)
[19] J. A. Haarwood, L. Mullins and A. R. Payne, J. Appl. Polym. Sci. **9**, 3011 (1965)
[20] J. A. Haarwood and A. R. Payne, J. Appl. Polym. Sci. **10**, 315, 1203 (1966)
[21] W. Kuhn and F. Grün, Koll. Z. Z. Polym. **101**, 248 (1946)
[22] M. Klüppel, Prog. Colloid Polym. Sci. **90**, 137 (1992)
[23] M. Klüppel and G. Heinrich, Macromolecules **27**, 3569 (1994)
[24] M. Klüppel, J. Appl. Polym. Sci. **48**, 1137 (1993)
[25] G. Heinrich and W. Beckert, Prog. Colloid Polym. Sci. **90**, 47 (1992)
[26] J. Kovac and C. C. Crabb, Macromolecules **15,** 537 (1982)
[27] N. R. Langley, Macromolecules **1**, 348 (1968)
[28] M. Klüppel, G. Heinrich and R. H. Schuster, Rubber Chem. Technol. **70**, 243 (1967)